Journal of Macromolecular Science, Part A
Publication details, including instructions for authors and subscription information:
http://www.informaworld.com/smpp/title~content=t713597274

Poly[Di(2,5-Dimercapto-1,3,4-Thiadiazole)-Palladium (II)] Complex: Synthesis, Characterization and DC Electrical Conductivity

Ali G. El-Shekeil[a]; Omar M. Al-Shuja'a[a]
[a] Faculty of Science, Department of Chemistry, Sana'a University, Sana'a, Yemen

To cite this Article El-Shekeil, Ali G. and Al-Shuja'a, Omar M.(2007) 'Poly[Di(2,5-Dimercapto-1,3,4-Thiadiazole)-Palladium (II)] Complex: Synthesis, Characterization and DC Electrical Conductivity', Journal of Macromolecular Science, Part A, 44: 9, 931 — 937
To link to this Article: DOI: 10.1080/10601320701424180
URL: http://dx.doi.org/10.1080/10601320701424180

Journal of Macromolecular Science®, Part A: Pure and Applied Chemistry (2007) **44**, 931–937

ISSN: 1060-1325 print/1520-5738 online
DOI: 10.1080/10601320701424180

Poly[Di(2,5-Dimercapto-1,3,4-Thiadiazole)-Palladium (II)] Complex: Synthesis, Characterization and DC Electrical Conductivity

ALI G. EL-SHEKEIL and OMAR M. AL-SHUJA'A
Faculty of Science, Department of Chemistry, Sana'a University, Sana'a, Yemen

Received and accepted February, 2007

A new poly[di(2,5-dimercapto-1,3,4-thiadiazole)-Pd(II)] complex (PDMT-Pd) was synthesized by the reaction of 2,5-dimercapto-1,3,4-thiadiazole (2 mmol) with palladium (II) chloride (1 mmol) in absolute ethanol under reflux for 24 hours. The products were characterized by elemental analyses, electronic spectra, FTIR spectroscopy, magnetic susceptibility, thermal analyses (TGA and DTA) and X-Ray diffraction. The DC electrical conductivity variation with temperature of the polymer-Pd (II) complex in the range 300–500 K was studied after annealing for 24 h at 100°C and after doping with 5% I_2, for comparison.

Keywords: poly[di(2,5-dimercapto-1,3,4-thiadiazole)-palladium(II)] complex; 2,5-dimercapto-1,3,4-thiadiazole; DC electrical conductivity; doping; thermal analysis; X-ray diffraction; activation energy

1 Introduction

The polymeric materials in different fields of application has led to some attractive research work in protective coatings, semi-conductors, catalysis and analytical applications (1–4). The 2,5-dimercapto-1,3,4-thiadiazole (DMT) and its metal-macromolecule complex attracted the attention of researcher for decades (5–9).

A new transition metal polymer complex was prepared by the reaction of DMT and the Pd(II) chloride in which the Pd(II) is in the backbone of the polymer chain. The isolated PDMT-Pd (II) was characterized by elemental analyses, electronic spectra, FTIR spectroscopy, magnetic susceptibility, thermal analyses (TGA and DTA), X-Ray diffraction and the DC electrical conductivity variation with temperature.

This polymer-palladium complex is interesting for various reasons. For example, the presence of donor atoms such as N and S in the polymer backbone contributes greatly to their thermal and environmental stability and enhances the electrical conductivity. Other important features include the nature of palladium-sulfur bonding interaction and the biological activity of this material.

Address correspondence to: Ali G. El-Shekeil, Faculty of Science, Department of Chemistry, Sana'a University, P. O. Box 12463, Sana'a. E-mail: shekeil@yemen.net.ye

The most important part of this work is the comparative study of the DC electrical conductivity. Two states of DC electrical conductivity were studied: the annealed and 5% I_2 doped states, with temperature variation in the range 300–500 K. The activation energies (Ea) were calculated from the DC electrical conductivity and thermal analyses.

2 Experimental

2.1 Chemicals

The 2,5-dimercapto-1,3,4-thiadiazole was purchased from Aldrich Chemicals, and was recrystallized twice before use. Palladium chloride was used as received from BDH. The solvents were reagent grade: 99% absolute ethanol, and DMF (BDH, Analar).

2.2 Synthesis of the Poly[di(2,5-dimercapto-1,3,4-thiadiazole)-Pd(II)] Complex

A solution of anhydrous palladium chloride (1 gm, 5.63 mmol) in a mixture of ethanol (25 ml) and methanol (25 ml) was added to a solution of 2,5-dimercapto-1,3,4-thiadiazole (1.69 gm, 11.26 mmol) in ethanol (25 ml). The mixture was refluxed with stirring for 24 h under a thin stream of nitrogen gas. The precipitated polymer was separated by filtration, then washed several times with hot ethanol and dried in the air for 24 h.

2.3 Instrumentation

The melting points were measured on an electrothermal melting point apparatus. The inherent viscosity of the polymer-metal was measured in DMSO using a suspended level Cannon-Ubbelohde viscometer. FTIR spectra were recorded using the KBr disc on a Shimadzu 8101 FTIR Spectrophotometer. The elemental (CHNS) analyses were performed on an Elemental Analyses system GmbH Varioel $V_{2.3}$ 1998 CHNS Mode. The UV and visible absorption spectra were measured in DMF using a PU 8800 UV-Visible Philips Automatic Scanning Spectrophotometer. The magnetic susceptibility was determined at room temperature by the Gouy Method (10). The thermal analyses (TGA and DTA) were carried out on a Shimadzu TGA-50 H and Shimadzu DTA-50 at 23 to 600°C under 20 ml nitrogen per minute and a heating rate of 10°C per minute. The X-ray diffraction was carried out on a Bruker Axs Da Advance, Germany. The electrical conductivity measurements were measured on a Keithley Picoammeter/Voltage Source Model 6487. Doping and annealing were performed as described previously (11).

2.4 Thermal Analyses of the Poly[di(2,5-dimercapto-1,3,4-thiadiazole)-Pd(II)] Complex

The thermal decomposition behavior of the poly[di(2,5-dimercapto-1,3,4-thiadiazole)-Pd] complex was investigated by thermogravimetric analysis (TGA).

For each step in the decomposition sequence, the parameters were determined as explained in the literature (12). The activation energy E_a was calculated from the slope of a plot of the Coats-Redfern equation (13) for the reaction order $n \neq 1$ which when linearized for a correctly chosen yields the activation energy from the slope;

$$\log\left[\frac{1-(1-\alpha)^{1-n}}{T^2(1-n)}\right] = \log\frac{ZR}{qE}\left[1-\frac{2RT}{E}\right] - \frac{E}{2.303RT}.$$

where: α = fraction of weight loss, T = temperature (K), n = order of reaction, Z = pre-exponential factor, R = molar gas constant, E_a = activation energy and q = heating rate. The order of reaction (n) is the one for which a plot of the Coats-Redfern expression gives the best straight line among various trial values of n that are examined, i.e., by trial and error for various trial values of n, estimated by the Horovitz-Metzger method (14).

3 Results and Discussion

3.1 Synthesis and Characterization

The PDMT-Pd was prepared by the reaction of 2,5-dimercapto-1,3,4-thiadiazole (2 mmol) with palladium chloride (II) (1 mmol) in a mixture of ethanol (25 ml) and methanol (25 ml). The mixture is stirred during 24 h under a thin stream of nitrogen gas, when the polymer-Pd(II) complex is formed. The dark brown solid is filtrated, washed with hot EtOH, then dried in the air for 24 h. The yield is 25%. The melting point is > 300°C. Elemental analysis as calculated for $C_4H_2N_4S_6Pd_2Cl_2 \cdot H_2O$ (Mol. Wt. = 600.24): C, 8.00%; H, 0.67%; N, 9.33%; S, 32.05%. Found: C, 8.34%; H, 0.81%; N, 8.96%; S, 31.70%. The inherent viscocity of the polymer-metal was found to be 0.53 dl/g showing a fairly low molecular weight (Scheme 1).

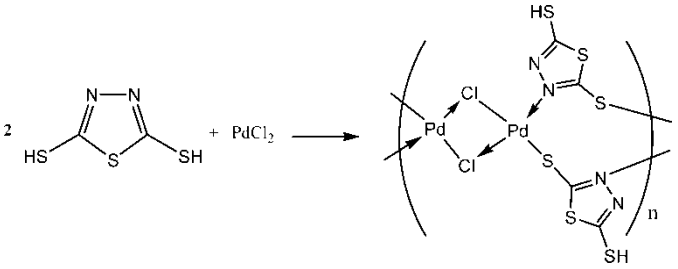

Sch. 1. The synthesis of the poly[di(2,5-dimercapto-1,3,4-thiadiazole)-Pd(II)] complex.

3.2 The FTIR Spectra

Figure 1 shows the FTIR spectra of the DMT and PDMT-Pd. The main FTIR bands are summarized in Table 1. The assigned absorption bands are consistent with the suggested structure.

The starting material (DMT) showed many bands and broadband absorptions in the 3100 – 1800 cm^{-1} range. These bands are attributed to overtones and combinations, except two bands that appeared at 2519 and 2485 cm^{-1},

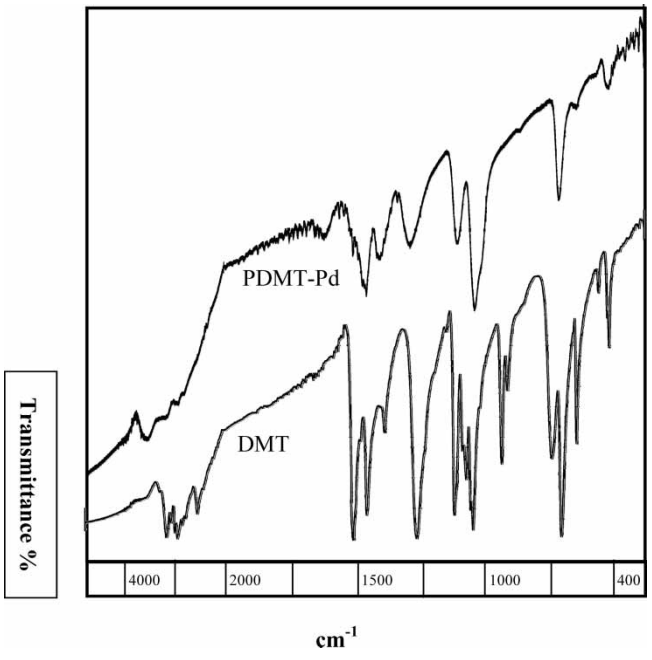

Fig. 1. The FTIR spectra of the poly[di(2,5-dimercapto-1,3,4-thiadiazole)-Pd(II)] complex.

Table 1. The main FTIR bands of the poly[di(2,5-dimercapto-1,3,4-thiadiazole)-Pd(II)] complex

	DMT	PDMT-Pd
ν(S-H)	2491 w	2491 vvw
ν_{as}(C═N)	1512 s	1512 w
ν_s(C═N)	1457, 1393 m	1470, 1414
δ ring	1273 s	1294
δ $(CNNC)_{ip}$	1128, 1098 w	1115
ν(N-N)	1085, 1055 m	1046
δ_{as} $(C\text{-}SH)_{ip}$	954 w	*
δ_s $(C\text{-}SH)_{ip}$	923 w	*
ν_{as}(C-S)	756,722 s	730
ν_s(C-S)	662 vw	*
ν_{as}(C-S')	585 w	580 vw
ν_s(C-S')	542 vw	542 vw
H_2O Bend. H_2O	—	3463 w 1628

v, very; w, weak; ν, stretch; δ, deformation; s, symmetric; as, antisymmetric; ip, in-plane, bend.; bending;*, not seen.

corresponding to the ν_{as}(S-H) and ν_s(S-H), respectively. The broadening of these features might be due to the presence of extensive hydrogen bonding of SH groups (15).

In the case of DMT, the stretch ν(S-H) weak band showed up weakly at (2491 cm^{-1}) and the deformation antisymmetric (δ_{as}) (C-SH) in-plane (ip) and *deformation symmetric* (δs) $(C\text{-}SH)_{ip}$ were noted also as weak bands at (948 cm^{-1}, 923 cm^{-1}), respectively. All these bands showed up as very weak bands in the product or disappeared. The noticeable shift in position of the ν_{as}(C═N), ν_s(C═N) and δ ring for the PDMT-Pd compared to DMT, is as assurance of the formation of the polymeric product. The bands observed in 440–500 cm^{-1} region are assignable to ν(M-N) (16).

The adsorbed water absorption bands appeared at 3000–3500 cm^{-1} for $\nu(H_2O)$ and the bending (H_2O) around (1630 cm^{-1}) (17).

3.3 Electronic Spectra

The main UV-visible absorptions of poly[di(2,5-dimercapto-1,3,4-thiadiazole)-Pd(II)] complex and DMT are summarized in Table 2.

Figure 2 illustrates the electronic spectra of the DMT and PDMT-Pd. The insertion in Figure 2 illustrates the electronic absorptions at 381, 460 and 490 nm confirming the d-d transitions of PDMT-Pd (II) complex.

The material showed three π-π^* (K-band) λ_{max} at 200–271 nm (50000–36900 cm^{-1}) and another four n-π^* (R-band) at λ_{max} 321–490 nm (31150–20400 cm^{-1}) characterized as ligand-to-Pd charge transfer. The charge transfer transition band showed up in the visible region for PDMT-Pd at 26250 cm^{-1}, 21750 cm^{-1} and 20400 cm^{-1}. The UV-visible absorption spectra of PDMT-Pd is typical of square-planar complex (21, 18). This proves the metal complex and that the bands are due to L → M (19, 20). The magnetic susceptibility measurements showed that the PDMT-Pd is diamagnetic.

3.4 Thermal Analysis

Thermogravimetric analysis is a very useful method to study the thermal decompositions of solid substances. In this study of the DC electrical conductivity, as the samples were subjected to temperature change, a change in the composition may lead to change of the measured quantities at the temperature range (25–225°C). To follow these changes, the material under study was subjected to differential thermal analyses (DTA).

The difference in the thermal decomposition behavior of the PDMT-Pd under a nitrogen atmosphere can be seen clearly in the thermogravimetric (TGA) curves. For each step in the decomposition sequence, it was possible to determine the following thermal parameters; T_i, T_f, TDTG, Δm and Ea, which are summarized in Table 3.

The TGA curves (Figure 3) obtained depict the decrease in sample mass with linear increase in treatment temperature. In the present investigation, the heating rate was fixed at 10°C min^{-1}. The 25–225°C range indicates that the PDMT-Pd lost the only one molecule of adsorbed water (21) that means it is stable in that range (first step). The range 225–512°C showed three steps as seen clearly from DTG.

The estimated and calculated mass losses were in reasonable agreement. In the range 225–303°C (second decomposition step), a mass loss of about 12.98% occurs. This

Table 2. The main UV-visible absorptions of poly[di(2,5-dimercapto-1,3,4-thiadiazole)-Pd(II)] complex

	π-π^*			n-π^*		
Compound	ν_{max} nm	ν_{max} (cm^{-1})	E_a(eV)	ν_{max} nm	ν_{max} (cm^{-1})	E_a(eV)
DMT	220	45500	5.6	355	28200	3.5
	230	43500	5.4			
	270	37040	4.6			
PDMT-Pd	200	50000	6.2	321	31150	3.9
	241	42500	5.1	381	26250	3.3
	271	36900	4.6	460	21750	2.7
				490	20400	2.5

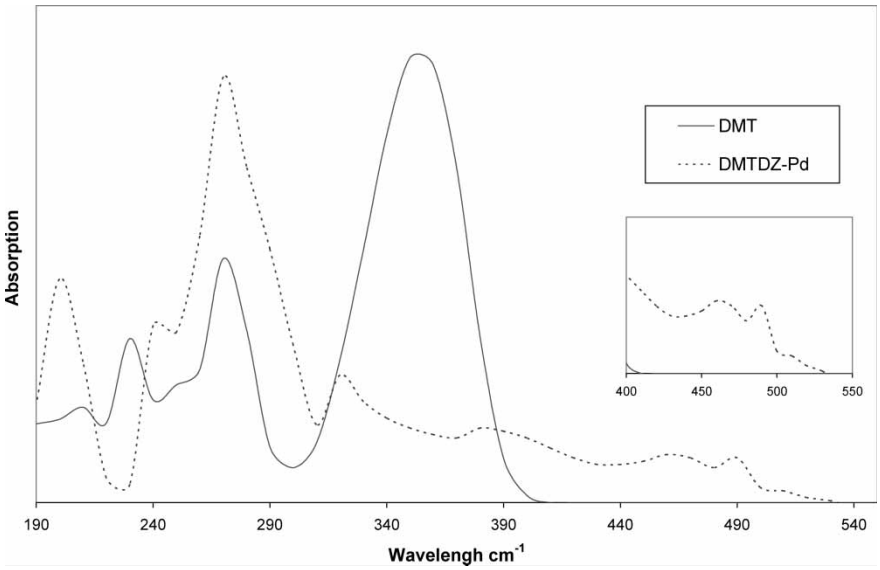

Fig. 2. The main UV-visible absorptions of poly[di(2,5-dimercapto-1,3,4-thiadiazole)-Pd(II)] complex.

reflects qualitatively the loss of 3 CN radicals (29.3% of backbone). The third decomposition step in the range 303–406°C is due to loss of 2 Cl and (9.8% of backbone maybe CN). The fourth step reflects the loss of 60.06%, which is the decomposition of the backbone (5S). The final residue was the corresponding palladium sulfide Pd_2S. These findings are also in good agreement with the behavior observed in the literature (22).

Table 3. The thermal gravimetric data of poly[di(2,5-dimercapto-1,3,4-thiadiazole)-Pd(II)] complex

Step no.	Wt. loss % found (calcd.)	TGA			Res. % found (calcd.)	E_a kJmol^{-1} (E_a eV)	React
		T_i/°C	T_f/°C	T_{DrTGA}			
1st	2.99 (3.00)	25	225	150, 226	97.01 (97.00)	11.63 (0.12)	H_2O
2nd	12.91 (13.00)	225	303	265	84.10 (84.00)	289.22 (2.30)	3 CN 29.3% bb
3rd	16.00 (16.14)	303	406	350	69.16 (67.86)	170.61 (1.77)	2Cl + CN 9.8% bb
4th	26.81 (26.71)	406	512	483	41.35 (42.15)	181.76 (1.88)	5S 60.06% bb

bb, backbone.

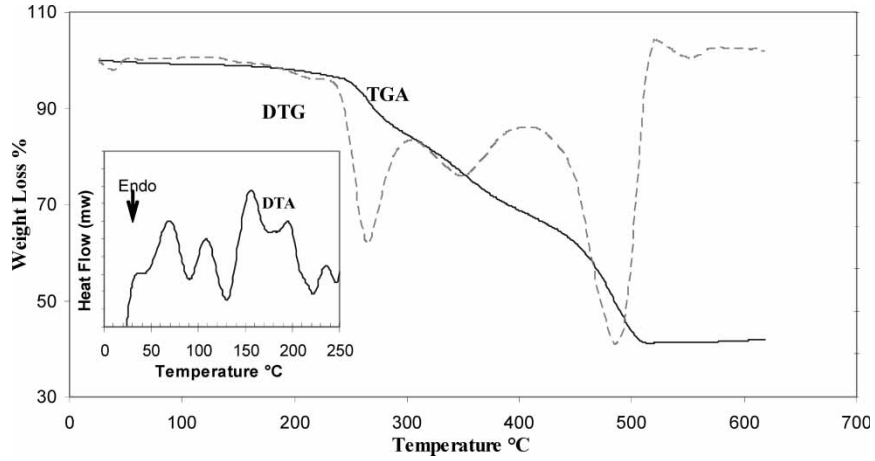

Fig. 3. The TGA and DTG curves of poly[di(2,5-dimercapto-1,3,4-thiadiazole)-Pd(II)] complex. The insert is the DTA in temperature range studied in the DC electrical conductivity.

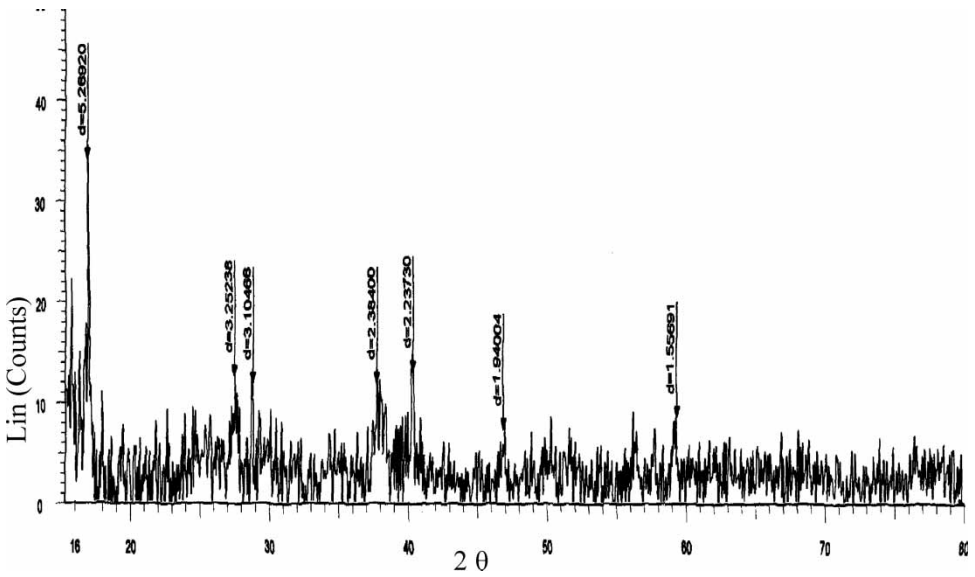

Fig. 4. The X-ray diffraction patterns of poly[di(2,5-dimercapto-1,3,4-thiadiazole)-Pd(II)] complex.

Complete details of decomposition and the associated activation energies are summarized in Table 3. Figure 3 illustrates the TGA and DTG curves of poly[di(2,5-dimercapto-1,3,4-thiadiazole)-Pd(II)] complex and the insert is the DTA in temperature range studied in the DC electrical conductivity.

3.5 X-ray Diffraction Patterns

The most direct method of investigation of the structure of the polymer (crystalline and amorphous) is the X-ray diffraction analyses (23). The X-ray diffractograph of the PDMT-Pd was determined at room temperature in the region $2\theta = 10^\circ - 80^\circ$ and illustrated in Figure 4. The X-ray diffractograph indicated that PDMT-Pd is likely amorphous structure.

3.6 DC Electrical Conductivity

The DC electrical conductivity of the PDMT-Pd was measured vs. $1000/T$ in the range 300–500 K. The effect of the annealing and the acceptor doping with 5% I_2 is measured and compared. The PDMT-Pd responded to heat by an increase in the electrical conductivity and behaved typically like of semiconductor materials (24, 25). The annealed and doped PDMT-Pd showed four and three stages or steps, respectively, that means, each step has its own activation energy.

The data of the DC electrical conduction measurements have been subjected to different treatments to investigate the conduction mechanism. Plots are made of $\log\sigma$ vs. $(T)^{-1}$, $(T)^{-1/2}$ and $(T)^{-1/4}$. Linear behavior of three plots is obtained. This means that the best fit could not be decided. This is due to the small temperature range of our experiments and the low sensitivity of our experimental electrical instrumentation (14).

Figure 5 shows the DC electrical conductivity vs. $1000/T$ of the annealed and doped (5% I_2) poly[di(2,5-dimercapto-1,3,4-thiadiazole)-Pd(II)] complex. The enhancement of DC electrical conductivity started for annealed and doped PDMT-Pd at ambient temperature from around 10^{-13} S cm^{-1}, in the two cases. The annealed and doped

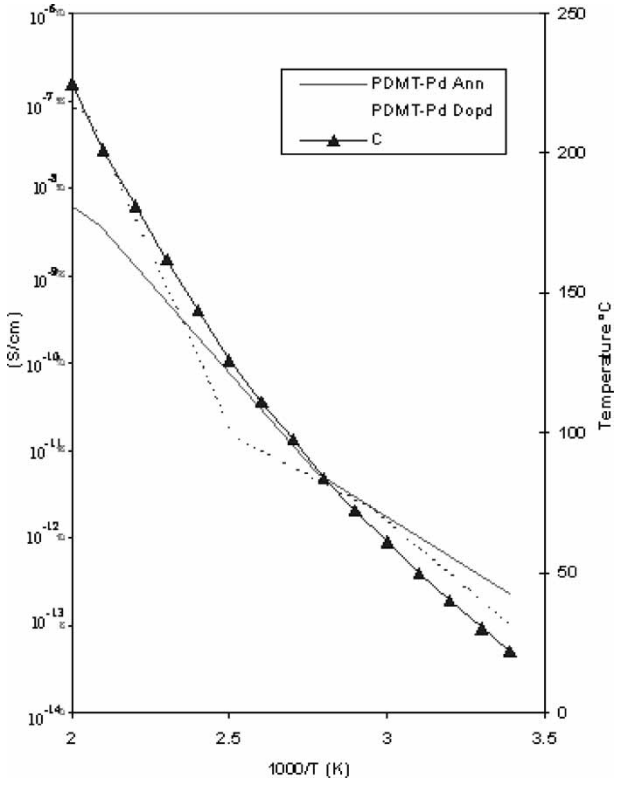

Fig. 5. The DC electrical conductivity vs. $1000/T$ of the annealed and doped (5% I_2) poly[di(2,5-dimercapto-1,3,4-thiadiazole)-Pd(II)] complex.

Table 4. The calculations for the bulk activation energies (E_a) at different temperature ranges of annealed and doped PDMT-Pd (II) complex

	Annealed (100°C/24 h)			Doped/annealed (5% I_2)		
Polymer-metal complex	T(°C)		E_a eV	T(°C)	E_a eV	
PDMT–Pd	22–87	0.8	BP-	22–69	0.6	P-
	87–204	0.4	P-	69–123	0.4	BP-
	204–225	0.4	BP-	123–209	1.6	VB
				209–225	0.4	BP-

PDMT-Pd gave a DC electrical conductivity at high temperature of 8.0×10^{-9} S cm^{-1} and 5.4×10^{-7} S cm^{-1}, respectively. The DC electrical conductivity at ambient temperature is almost similar for the annealed and doped DMT-Pd; while, the highest DC electrical conductivity at higher temperature is noticed for the doped PDMT-Pd by about two orders of magnitude. The enhancement of DC electrical conductivity of the doped PDMT-Pd compared to the annealed PDMT-Pd is attributed to the doping with acceptor I_2, that is the normal case (10, 26, 27).

3.7 Activation Energies

The carriers available for the DC electrical conductivity are electrons and holes. The calculations for the bulk activation energies (Ea) at different temperature ranges for all the segments of the curves of the annealed and doped PMDT-Pd are summarized in Table 4.

The annealed PDMT-Pd gave three activation energies, while the doped PDMT-Pd gave four segments and thus four activation energies. All these segments are due to physical reactions (phase transitions or chain conformation) as shown in DTA. These are in accordance with the small peaks near these ranges as a T_i or T_{max} in the DTA, which does not correspond to weight loss in the TGA (28, 29). Consequently, there is some kind of phase transition across this specific temperature. The stepped behavior was observed in the doped polymer more than in the annealed. This is obviously due to the decrease of crystallinity of the polymers (30).

Figure 6 shows the energy schematic model based on the band theory. In this case, the bulk energy gap (BEG) is about 1.6 eV. This is the highest activation energy obtained.

For the annealed PDMT-Pd, the first segment in the range (22–87°C) and the third segment in the range (204–225°C) are due to the excitation from the upper levels of the negative bipolaron (BP^-), which is 0.4 eV below the bulk conduction band (BCB). The second segment (87–204°C) is due to soliton (S^-) level excitation (i.e. in the middle of (BEG) (31)) which is about 0.8eV.

For the doped PDMT-Pd, The first segment (22–69°C), is due to excitation from the upper level of negative polaron (P^-), which is ~0.6 eV. The second (69–123°C) and fourth (209–225°C) segments are due to the excitation from (BP^-), which is 0.4 eV. The third segment (123–209°C) is due to the excitation from the bulk valance band (BVB), which is ~1.6 eV.

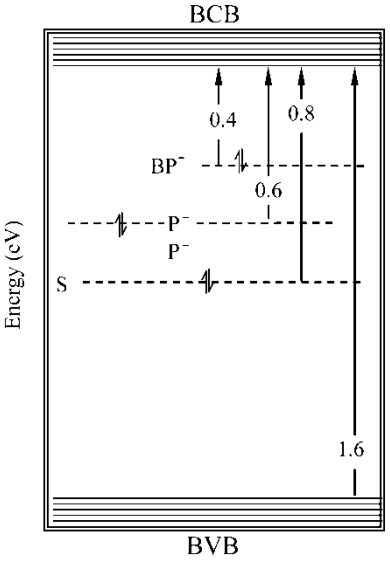

Fig. 6. The proposed energy schematic model based on the band theory of PDMT-Pd.

4 Conclusions

The following points can be concluded from this work:

1. The reaction of the 2,5-dimercapto-1,3,4-thiadiazole with anhydrous palladium (II) chloride formed polymer-Pd complex of the type $[L_2M_2Cl_2]_nH_2O$. The chemical and physical properties are studied.
2. The correlations between CHNS analysis, TGA, DTA, X-ray diffraction and DC electrical conductivity are noticed and followed.
3. The polymer-metal complex is thermally stable up to 500 K.
4. The electrical conductivity of the PDMT-Pd complex, whether annealed or doped, increased with increasing temperature. This is mainly due to the variation of the carrier concentration with temperature as in the case of semiconductors.
5. The PDMT-Pd complex has palladium ions in its backbone. Thus, it is doped internally, so the doped PDMT-Pd

complex is only two orders of magnitude higher in DC electrical conductivity than the annealed state.

6. Thermogravimetric analysis of PDMT-Pd showed all steps in the decomposition sequence; the estimated and calculated mass losses were in reasonable agreement and are in good agreement with the behavior observed in the literature.

5 Acknowledgments

The authors gratefully acknowledge the financial support from TWAS (Grant 04-053 LDC/CHE/AF/AC).

6 References

1. Nalwa, H.S. *Handbook of Organic Conductive Molecules and Polymers*; John Wiley: New York, Vol. 2, 1997.
2. Kiess, H.G. *Conjugated Conducting Polymers, Springer Series in Solid State Science*; Springler: Berlin, Vol. 102, 1992.
3. Kuzmany, H., Mehring, M. and Roth, S. *Electronic Properties of Polymers and Related Compounds, Springer Series in Solid-State Sciences*; Springer: Heidelberg, Vol. 63, 1985.
4. Mort, J. and Pfister, G. *Electronic Properties of Polymers*; John Wiley: New York, 1982.
5. Jamaluddin, A.M. and Mosaddeque-Al, M. (2001) *Talanta*, **55**, 43–49.
6. Shouji, E. and Butty, D. (1999) *Langmuir*, **15**, 669–673.
7. Jinxia, L., Zhan, H. and Zhou, Y. (2003) *Electrochemistry Communications*, **5**, 555–560.
8. Farng, L.O., Horodysky, G.A. and Olszewski, W.F. US Patent 1990; 137(5): 649.
9. Oyama, N., Tastuma, T. and Sotomura, T. (1997) *Journal of Power Sources*, **68**, 135–138.
10. Cotton, F.A. and Wilkinson, G. *Advanced Inorganic Chemistry*, 3rd Edn.; Wiley: New York, Vol. 594, 1962.
11. El-Shekeil, A., Khalid, M. and Al-Yusufy, F. (2001) *Macromol. Chem. and Phys.*, **202**, 2971–2983.
12. Al-maydama, H., El-Shekeil, A., Khalid, M.A. and Al-Karbouly, A. (2006) *Ecl. Quím. São Paulo*, **31(1)**, 45–52.
13. Coats, A.W. and Redfern, J.P. (1964) *Nature*, **68**, 201–208.
14. Horovitz, H.H. and Metzger, G. (1963) *Anal. Chem.*, **35**, 1464–8.
15. Bellamy, L.J. *The Infrared Spectra of Complex Molecules*; Wiley: New York, Vol. 1, 395, 1975.
16. Cherayath, S.R., Alice, J. and Chathakudam, P. (1990) *Transition Met. Chem.*, **15**, 449–453.
17. El-Shekeil, A., Khalid, M.A., Al-Maydama, H. and Al-Karbooly, A. (2001) *European Polymer Journal*, **37**, 575–581.
18. Lever, A.B.P. *Inorganic Electronic Spectroscopy*; Elsevier: New York, 1986.
19. Rastogi, D. and Sharma, K. (1997) *J. Inorg. Nucl. Chem.*, **36**, 2219–2223.
20. Khalid, M.A., El-Shekeil, A.G. and Al-Yusufy, F.A. (2001) *European Polymer Journal*, **37**, 1423–1432.
21. Donia, A.M., Al-Ansi, T.Y. and Othman, M.Q. (1997) *J. Thermal Analysis*, **50**, 857–865.
22. Merdivan, M., Karipcin, F., Kulcu, N. and Aygun, R.S. (1999) *J. Thermal Analysis and Calorimetry*, **58**, 551–557.
23. Perepechk, I.I. *An Introduction to Polymer Physics*; Mir Publishers: Moscow, Vol. 31, 1981.
24. Katon, J.E. *Organic Semiconducting Polymers*; Marcel Dekker: New York, 40–41, 1968.
25. Nalwa, H.S. *Handbook of Organic Conductive Molecules and Polymers*; John Wiley: New York, 2, 763, 1997.
26. Par, S.B., Kim, H., Zin, W.C. and Jung, J.C. (1993) *Macromolecules*, **26**, 1627–1635.
27. Saegusa, Y., Ozeki, Y., Harada, S. and Nakamura, S. (1994) *Macromol. Chem. Phys.*, **195**, 3189–3195.
28. Sanyal, T.K. and Dass, N.N. (1980) *J. Inorganic Nuclear Chemistry*, **42**, 811–813.
29. Beoerio-goates, J. and Callanan, J.E. Differential thermal method. *Determination of Thermodynamic Properties, Physical Methods of Chemistry*, 2nd Edn.; Rossiter, B.W. and Baetzold, R.C. (eds.); John Wiley and Sons: New York, 4, 621–717, 1992.
30. El-Shekeil, A.G., Al-Yusufy, F.A. and Saknidy, S. (1997) *Polymer International*, **42**, 39–44.
31. Nalwa, H.S. (ed.) *Handbook of Organic Conductive Molecules and Polymers*; John Wiley: New York, Vol. 2, 16, 1997.